

Article

Timing of Ore Mineralisation in Deposits of the Baikal-Muya Belt and the Barguzin-Vitim Super-Terrain (Transbaikalie)

Vadim A. Vanin ^{1,2}, Alexei V. Ivanov ^{1,*} , Viktor A. Gorovoy ¹, Alexander E. Budyak ^{2,3} and Nikolay S. Bortnikov ⁴

¹ Institute of the Earth's Crust, Siberian Branch of the Russian Academy of Sciences, 664033 Irkutsk, Russia; vanin_geo@mail.ru (V.A.V.); vagorovoi@mail.ru (V.A.G.)

² Siberian School of Geosciences, Irkutsk National Research Technical University, Lermontova, 83, 664074 Irkutsk, Russia; budyak@igc.irk.ru

³ A.P. Vinogradov Institute of Geochemistry, Siberian Branch of the Russian Academy of Sciences, 664033 Irkutsk, Russia

⁴ Institute of Geology of Ore Deposits, Petrography, Mineralogy and Geochemistry, Russian Academy of Sciences, 119017 Moscow, Russia; bns@igem.ru

* Correspondence: aivanov@crust.irk.ru

Abstract: The study was aimed at dating of Au ores from the Yubileinoe, Irokinda and Uryakh deposits located in the Baikal-Muya fold belt and Pb-Zn ores from the Ozernoe deposit in the Barguzin-Vitim super-terrain (Transbaikalia, Russia). The ⁴⁰Ar/³⁹Ar ages on pyrite-encapsulated sericite of gold-bearing quartz sampled from veins in the Yubileinoe, Irokinda and Uryakh deposits are 265 ± 33 Ma, 276 ± 13 Ma and 287 ± 7 Ma, respectively. The age of disseminated mineralisation in the Ozernoe deposit is 329 ± 19 Ma. The results of this study and previously published data suggest two stages of ore mineralisation at Transbaikalia: 330–320 Ma for the disseminated mineralisation and 290–270 Ma for the vein mineralisation. Irrespective of the location and the nature of the host rocks, the former and the latter mineralisation are transiently associated with the initial and final stages of the emplacement of the Angara-Vitim granitic batholith. The granitoids provided heat and possibly fluids, while Au, Pb and Zn were sourced from the host rocks. Gold deposits to the north and south of the batholith are generally older and younger, respectively, and were formed by different geological processes.

Keywords: ⁴⁰Ar/³⁹Ar dating; ore deposits; Baikal-Muya super-terrain; Barguzin-Vitim super-terrain; Yubileinoe; Irokinda; Uryakh; Ozernoe; Mukodek



Citation: Vanin, V.A.; Ivanov, A.V.; Gorovoy, V.A.; Budyak, A.E.; Bortnikov, N.S. Timing of Ore Mineralisation in Deposits of the Baikal-Muya Belt and the Barguzin-Vitim Super-Terrain (Transbaikalie). *Minerals* **2024**, *14*, 1158. <https://doi.org/10.3390/min14111158>

Academic Editors: Xiaoyong Yang and Wenhua Ji

Received: 4 October 2024

Revised: 12 November 2024

Accepted: 14 November 2024

Published: 15 November 2024



Copyright: © 2024 by the authors. Licensee MDPI, Basel, Switzerland. This article is an open access article distributed under the terms and conditions of the Creative Commons Attribution (CC BY) license (<https://creativecommons.org/licenses/by/4.0/>).

1. Introduction

Determining the age of an ore deposit is often difficult for a number of reasons. Firstly, ore formation can be a multistage process and, for example, dating the host rock may not provide an answer to the age of the ore itself. Secondly, it is difficult from an analytical point of view because the ore minerals cannot always be dated by routine geochronological tools, while spatially associated minerals suitable for dating may not have crystallized synchronously with the ore. Recently, it has been suggested that pyrite, which is often an important host for gold mineralisation, can be dated by the ⁴⁰Ar/³⁹Ar method on encapsulated sericite grains [1–4]. For example, at the Mukodek gold-ore field in the Baikal-Muya Belt (northern Transbaikalia, Siberia, Russia), two stages of mineralisation were identified using such an approach: fine-grained (first generation) and coarse-grained (second generation) pyrite yielded ages of 321 ± 1.9 Ma and 284 ± 15 Ma, respectively [4]. These ages correspond to the early and late stages of the Angara-Vitim batholith emplacement [5–8], suggesting a link between felsic magmatism and gold ore formation in Transbaikalia in the Late Palaeozoic (Figure 1). Understanding the “scenario” of gold mineralisation in the Mukodek gold deposit, whose reserves are relatively small, may help to elucidate the mineralisation history of larger ore zones in the Baikal-Muya Belt and other tectonic structures

of Transbaikalia [9]. This paper presents some new results of $^{40}\text{Ar}/^{39}\text{Ar}$ dating results of pyrite-encapsulated sericite from three deposits in the Baikal-Muya Belt (BMB) and one deposit in the Barguzin-Vitim super-terrain of the Central Asian Orogenic Belt (CAOB), and reviews available geochronological data for some of these and other deposits (Figure 1). All these deposits are characterised by spatial association with the Early Carboniferous–Early Permian Angara-Vitim batholith [5–8] (Figure 1). The results of our research show that the deposits under consideration were formed in two stages and are coeval with this batholith, in contrast to the gold deposits to the north and south, which were formed in the Silurian–Early Carboniferous [10–13] and Jurassic–Early Cretaceous [14,15], respectively (Figure 1).

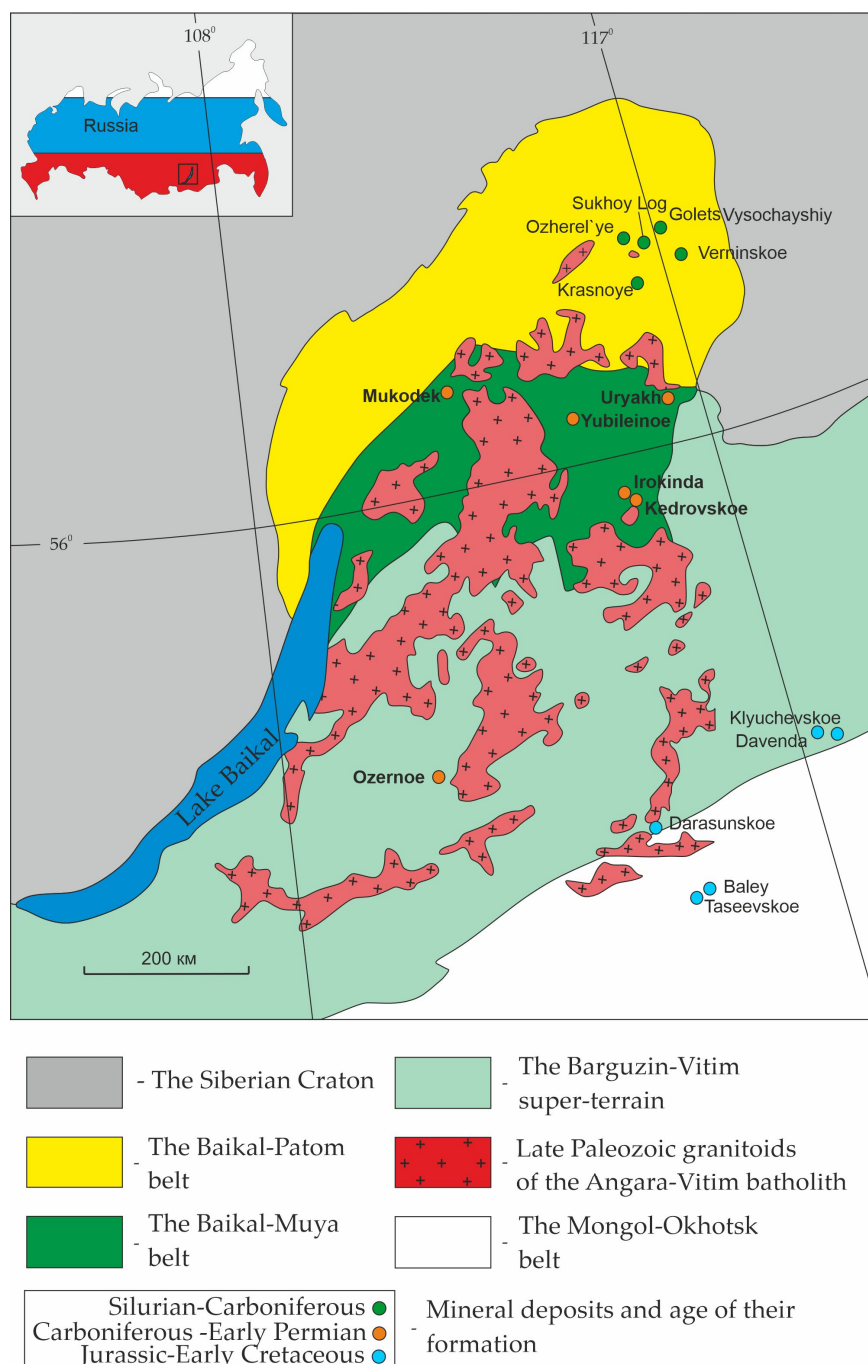


Figure 1. Schematic locations of polymetallic Ozernoe deposit and gold (other named) deposits in Transbaikalia. Deposits studied in this paper are marked in bold.

2. Geological Characteristics of the Deposits

In general, the Yubileinoe, Uryakh and Irokinda deposits are located within the Baikal-Muya Belt (BMB) (Figure 1). These deposits have been classified as belonging to mesothermal formations with low-sulphide gold-quartz and gold-(pyrite)-galenite-sphalerite (\pm chalcopyrite faded ore) mineralogical types. Alteration zones are represented by disseminated and veined ore types. The main gold ore of these deposits is hosted in quartz veins. Vein-disseminated ore is poorly investigated for gold and is generally considered to be less profitable.

The Yubileinoe deposit is located in the central part of the Baikal-Muya belt (Figure 1). The rocks are metarhyolites, metadacites and metasediments of a Neoproterozoic volcanic arc intruded by post-collisional metagabbro and plagiogranites of uncertain age and by granitic dikes of the Konkudero-Mamakan complex (320–280 Ma [6]) (Figure 2). The alteration zone is hosted in schists and mylonites that have developed along a fault on metamorphosed volcanic-sedimentary rocks (Figure 2).

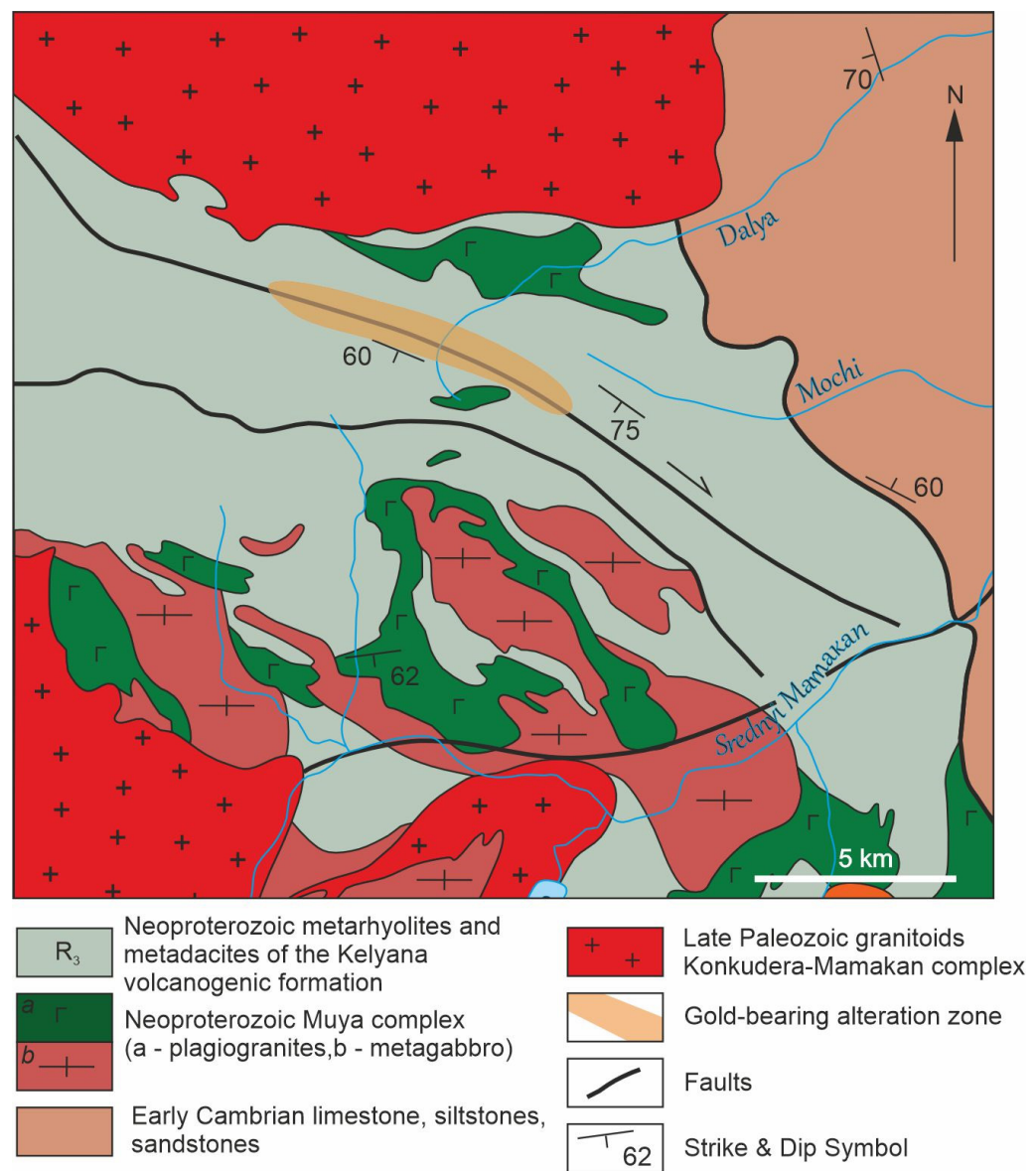


Figure 2. Geological map of the Yubileinoe deposit (this study).

The vein-type ore at the Yubileinoe deposit is represented by quartz and quartz-carbonate veins with a total length of up to 360 m and a thickness of 0.6–1.6 m (Figure 3). The main minerals in the veins are quartz (80%–90%) and carbonates (10%–20%). There are four generations of quartz in four mineral associations (from old to young): quartz, quartz-pyrite, quartz-sphalerite-chalcopyrite-galenite and gold-telluride-quartz [16]. The disseminated ore type (Figure 4a) is represented by albite-chlorite-quartz-sericite-carbonate and sericite-quartz-chlorite-carbonate metasomatic rocks. The former are known in Russian geological literature as beresites, while the latter are known internationally as listvenites. The gold-bearing veins (Figure 4b) cut the metasomatic rocks of the disseminated formation (Figure 3). The disseminated- and vein-type ores contain rounded (Figure 4a) and rectangular (Figure 4b) pyrites belonging to the first and second generations.

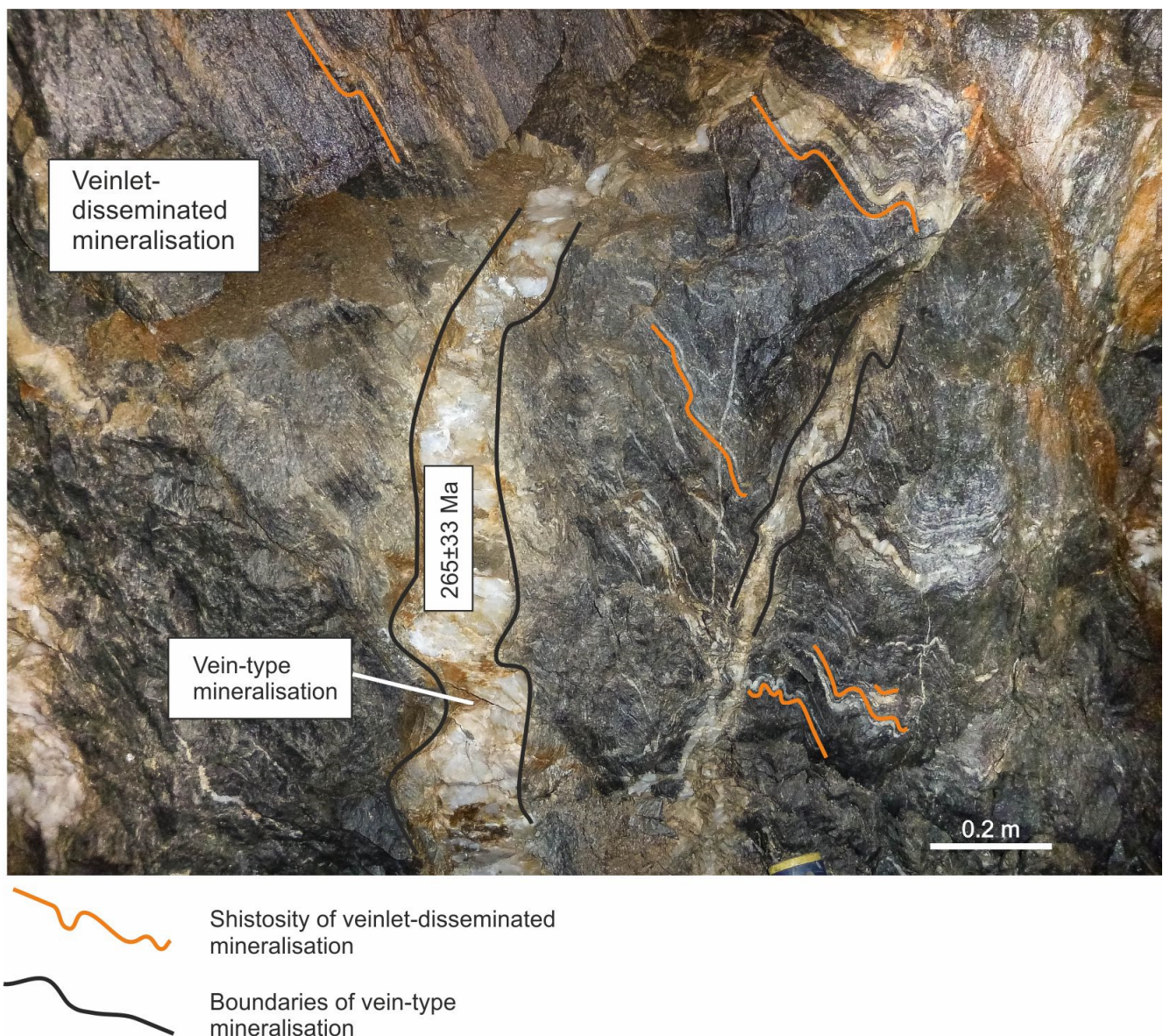


Figure 3. Geological relationship of vein and disseminated ore types of the Yubileinoe deposit. The $^{40}\text{Ar}/^{39}\text{Ar}$ age of pyrite-encapsulated sericite is shown (this study).

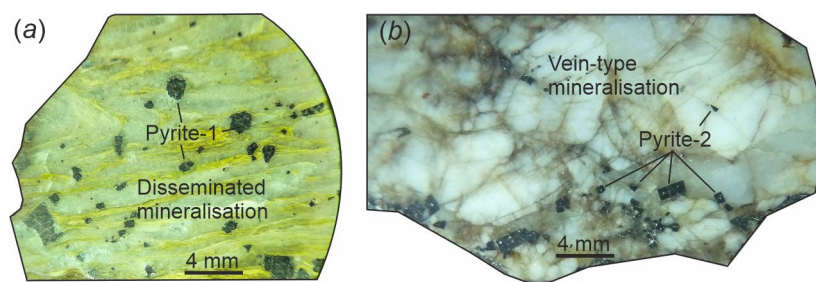


Figure 4. Examples of pyrites of the first (a) and second (b) generation from different type ores of the Yubileinoe deposit.

Ore minerals, mainly pyrite, and less commonly chalcopyrite, galenite, sphalerite, fahlore (tetrahedrite), tellurides (altaite, petzite, hessite, melonite, etc.) and native gold make up to 3%. Two generations of pyrite have been identified. The first generation of pyrite is restricted to the disseminated ore. It has rounded grains with a size of 0.05–0.07 mm, sometimes with formed grains close to octahedral. The second generation of pyrite has the euhedral, cubic or free forms with a typical grain size of 0.1–5 mm. It is found in both the disseminated- and vein-type ores (Figure 4a,b).

Gold in the veins occurs either in native form (0.01–3 mm in size) or as tellurides (petzite and calaverite) associated with sulphides. Gold concentrations in pyrite separated from the vein and ore disseminated from the vein reach up to 70 ppm and 15 ppm, respectively.

The Uryakh deposit is located in the northern BMB on the border of the Baikal-Patom Belt (BPB) (see Figure 1). Gold reserves are estimated at ~10 metric tonnes [17]. Its geological units include Neoproterozoic terrigenous-carbonate rocks, Neoproterozoic metagranitoids, metagabbro, metavolcanics and Upper Paleozoic mafic and felsic dikes. The host rocks are terrigenous carbonates, metagranitoids, metagabbro and metavolcanic rocks. The deposit is located in the zone of the regional Syulban fault (Figure 5).

The amount of sulphide in the ores reaches up to 1%. Similar to the Yubileinoe deposit, the Uryakh deposit has two generations of pyrite: the first generation is restricted to veinlets and the second generation occurs in both ore types (Figures 6 and 7). Gold occurs in both ore types within either quartz or second-generation pyrite (Figure 8b,c).

The vein type at the Uryakh deposit (Figures 6 and 7) is represented by quartz veins with a total length of up to 100 m and a thickness of up to 3 m. The disseminated ore type (Figures 6 and 7) is represented by beresites composed of sericite, ankerite, quartz and pyrite. The veins cut the structure of the veinlets (Figure 6a,b).

For sericite collected from the exocontact of the gold-quartz vein in terrigenous-carbonate rocks, the ages constrained by Rb-Sr and $^{40}\text{Ar}/^{39}\text{Ar}$ dating are 281 ± 5 Ma and 275 ± 6 Ma, respectively [18]. The sericite used for dating was collected from the contact zone with the vein and is therefore likely to represent the age of the vein formation.

The Irokinda field is located in the South Muya BMB tectonic block (Figure 1). Gold reserves are estimated at ~24 metric tonnes [16]. The geological structure includes Neoproterozoic gneisses, amphibolites, metagabbro, granitoids and late Palaeozoic felsic and intermediate composition dikes. Neoproterozoic gneisses and granitoids host gold zones [19] (Figure 9).

The ore-controlling structure is the Kelyansky Fault. Over one hundred gold-bearing quartz veins have been identified in the deposit. The veins range in length from 60 to 400 m and in thickness from 0.4 to 5.5 m. The sulphide content of the quartz veins does not exceed 1.5%. Pyrite (Figure 8d–f) in the quartz veins is dodecahedral and cubic, ranging in size from 0.3 to 3 mm, forming nest-vein clusters and disseminated.

The disseminated type is represented by tectonised beresites and listvenites with quartz veins and disseminated sulphide mineralisation. Gold is common in vein-disseminated and vein-type ores in quartz and pyrite. Gold is rarely found in fractures in pyrite of vein-type ores (Figure 8d,e).

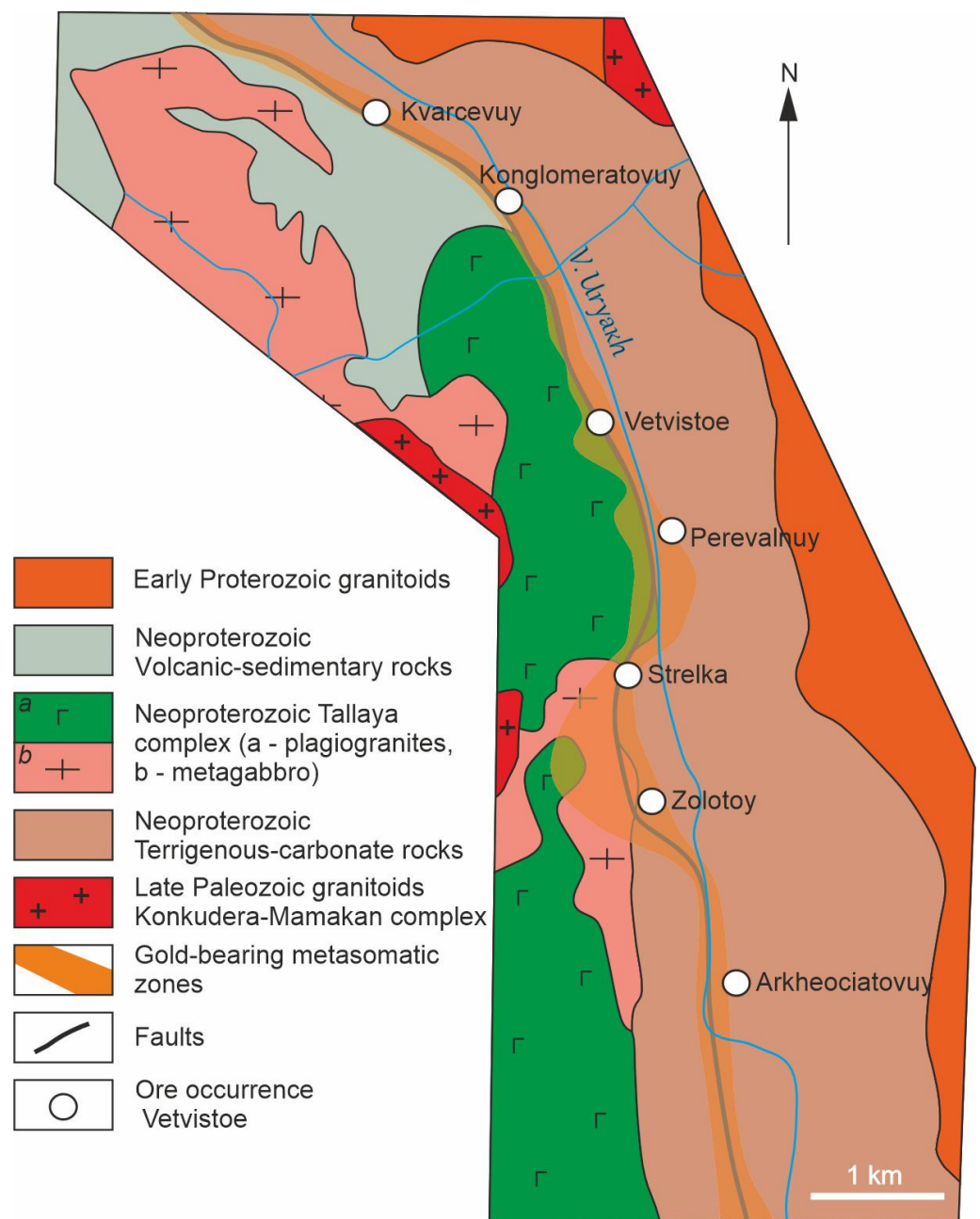


Figure 5. Geological map of the Uryakh deposit (this study).

The age of the alteration zone is determined by K-Ar and Rb-Sr dating of sericite from metasomatic zones within the deposit: 271 ± 5 Ma and 275 ± 7 Ma, respectively [20]. The age of sericite from quartz veins determined by the $^{40}\text{Ar}/^{39}\text{Ar}$ method is 268 ± 5 Ma [21].

The Kedrovka field is located in the South Muya BMB tectonic block [20] (Figure 1). Gold reserves are estimated at ~28 metric tonnes [16]. The geological structure includes Neoproterozoic metasedimentary rocks, 800–750 Ma granodiorites [9,22], 735 Ma metagabbro [23], and Paleozoic dikes and massive granites. Metasediments, granites and gabbro of the Muya Complex host gold (Figure 10).

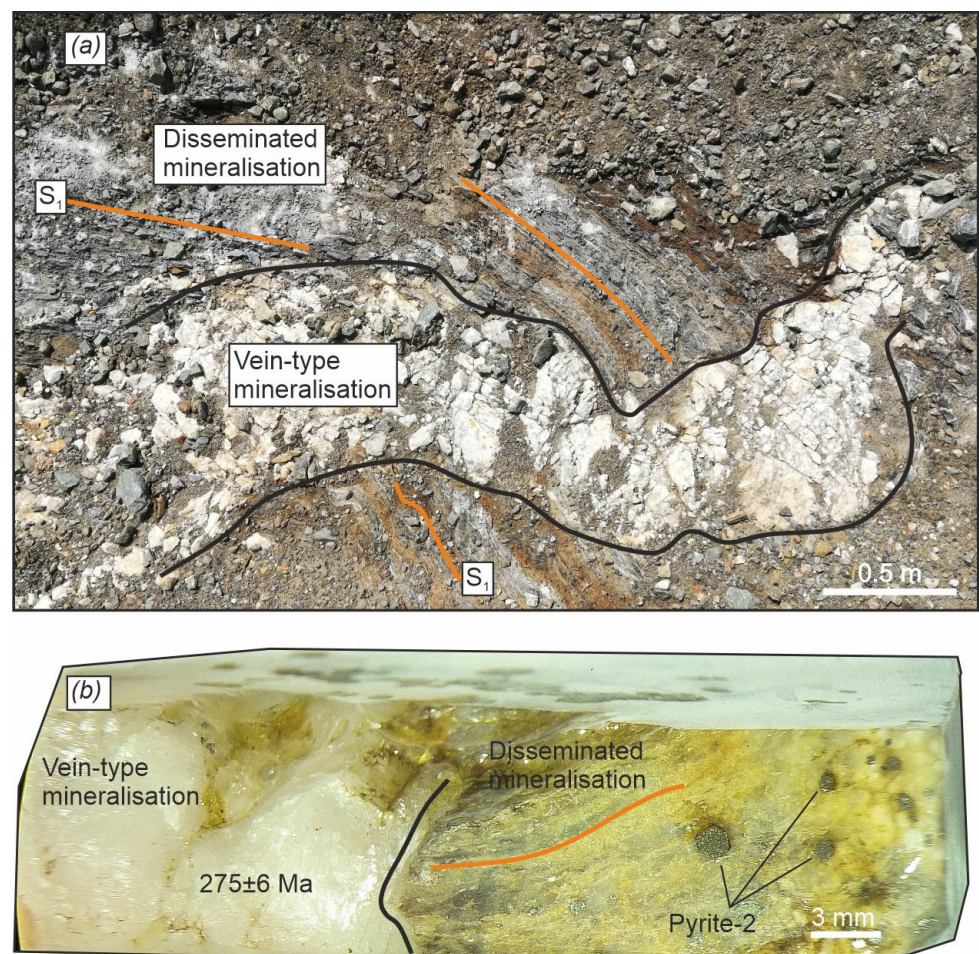


Figure 6. Geological relationship of veins and disseminated ore types at the Uryakh deposit. (a) photo of a trench; (b) photo of a polished section. The $^{40}\text{Ar}/^{39}\text{Ar}$ age of pyrite-encapsulated sericite is shown [18].

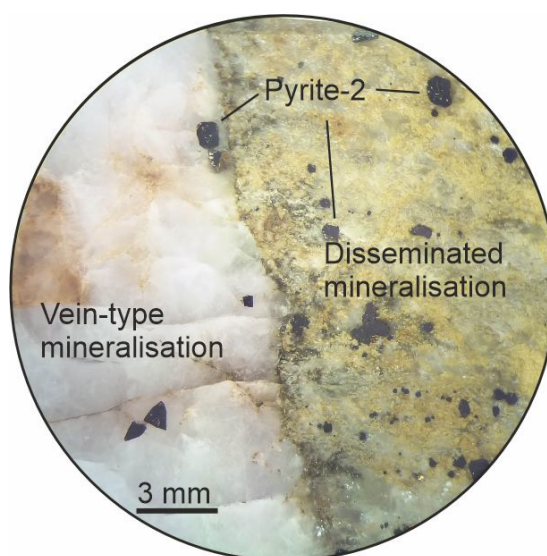


Figure 7. Examples of pyrites of the second generation from different ore types of the Uryakh deposit.

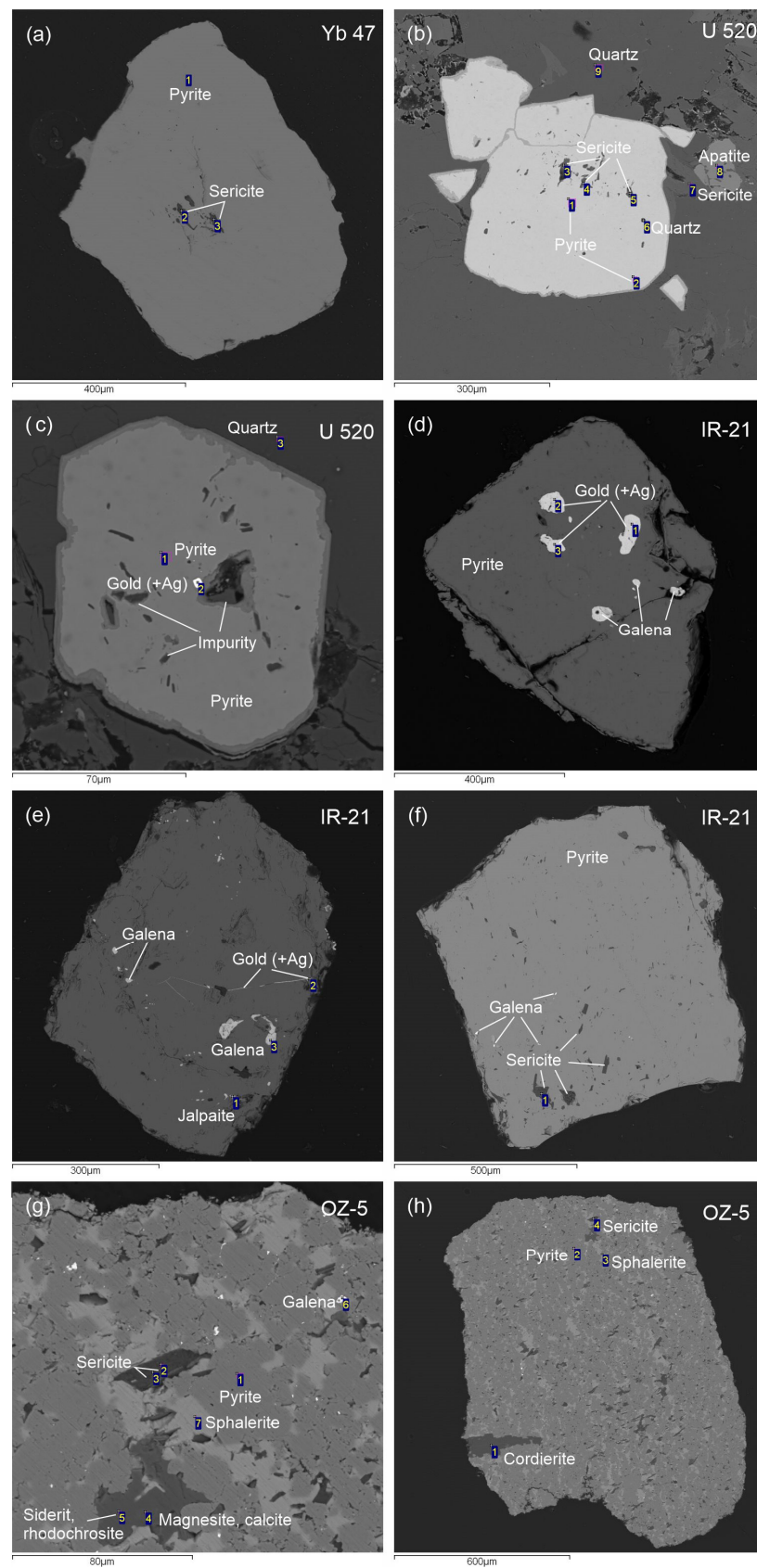


Figure 8. Representative backscattered electron images for deposits Yubileinoe (a), Uryakh (b,c), Irokinda (d–f) and Ozernoe (g,h).

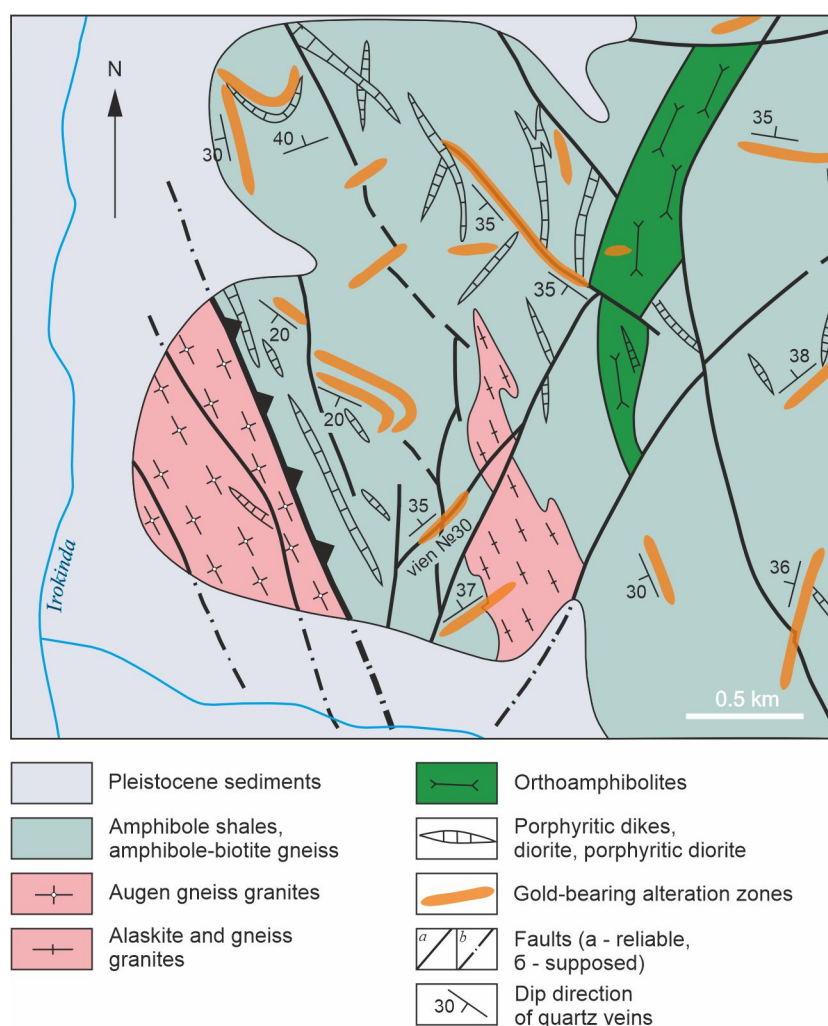


Figure 9. Geological map of the Irokinda deposit (modified after [19]).

The ore-controlling structure is the Tuldun Fault. Ore zones are represented by quartz-pyrite association with scheelite and gold-polysulphide (gold-sphalerite-galenite) association. Scheelite is common in the vein quartz. In the work of [24], near-metasomatites and sericitolite in vein quartz were analysed by the Rb-Sr method, which most likely gave the age of the quartz veins. In [20], a bulk sample of the ore zone was analysed without separation of the vein type and the disseminated vein type.

The Mukodek ore field is described in [4,25]. Gold reserves are estimated at ~20 metric tonnes [16]. It is hosted within island arc formations—volcanogenic-sedimentary sequence and metagabbroids that are intruded by 600 Ma plagiogranites (unpublished author's data). The ore-controlling structure is a fault (Figure 11). In the ore field, alteration zones are represented by disseminated- and vein-type ores. Both disseminated and vein types are of practical importance. The disseminated ores are sericite—chlorite—ankerite—albite—quartz. The vein-type ores are represented by quartz-carbonate veins. The vein-disseminated ores are folded in the right-lateral folds. The position of the vein-type ore relative to the vein-disseminated ore is inclined at an angle close to the angle of the fold axis (Figure 12).

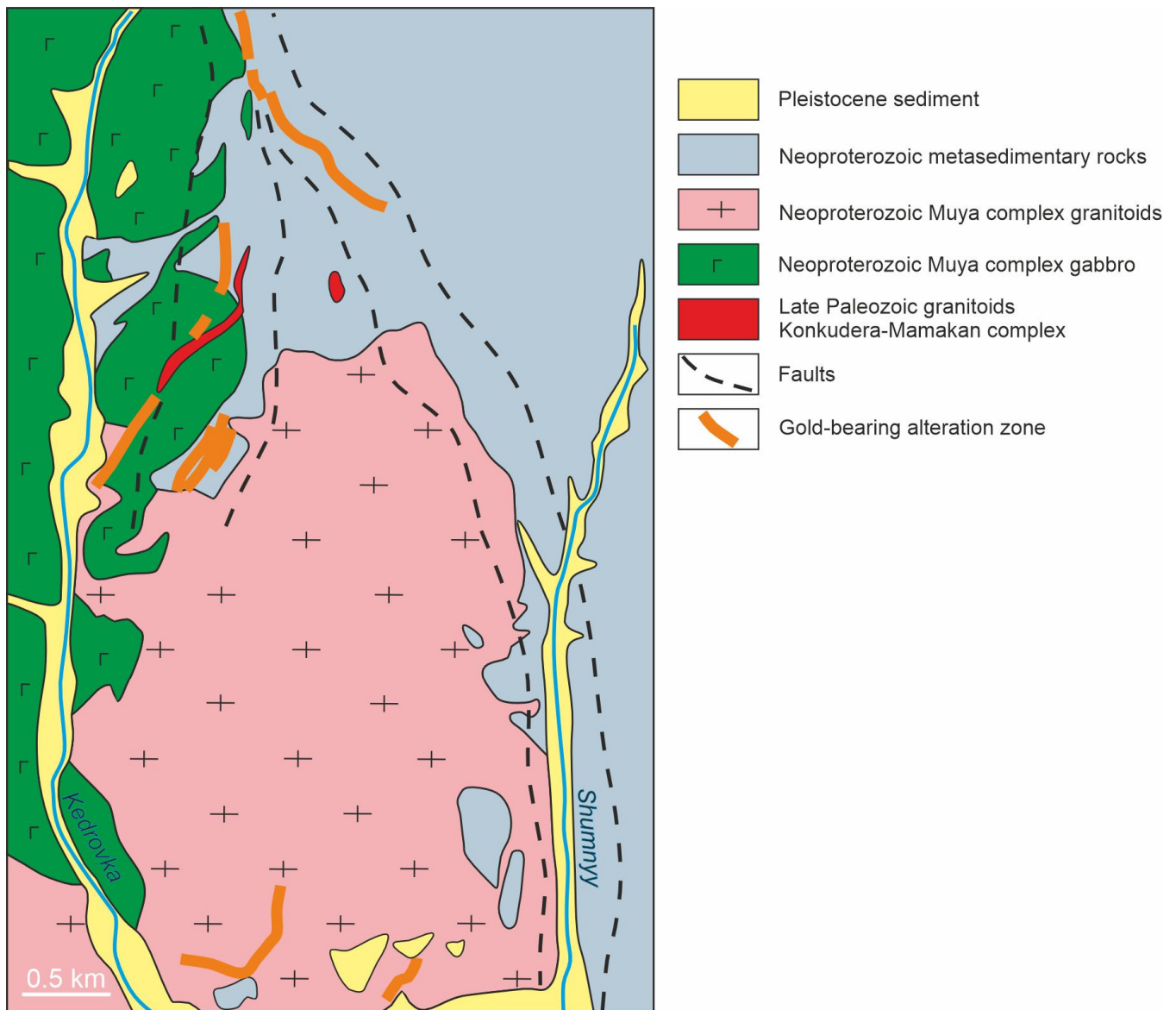


Figure 10. Geological map of the Kedrovskoe deposit (modified after [22]).

The alteration zone contains two generations of pyrite. Pyrite-1 is widespread in the vein-disseminated ore. Pyrite-2 is found in the vein type of ore. Pyrites-1 are <1 mm in size, while those from the veins are up to a few cm in size. $^{40}\text{Ar}/^{39}\text{Ar}$ ages of 321 ± 2 Ma and 284 ± 15 Ma were obtained for pyrite-1 and pyrite-2, respectively [4].

The Ozeroye Pb-Zn deposit is hosted in Early Cambrian sedimentary volcanic rocks [26]. The Pb-Zn reserves are estimated at 165 million metric tonnes [27]. The alteration zone is controlled by an asymmetric synclinal fold and north-east trending faults (Figure 13). The alteration zone of the deposit is represented by the disseminated type. The genesis of the deposit is controversial, either volcanogenic-sedimentary [28] or hydrothermal-metasomatic [29].

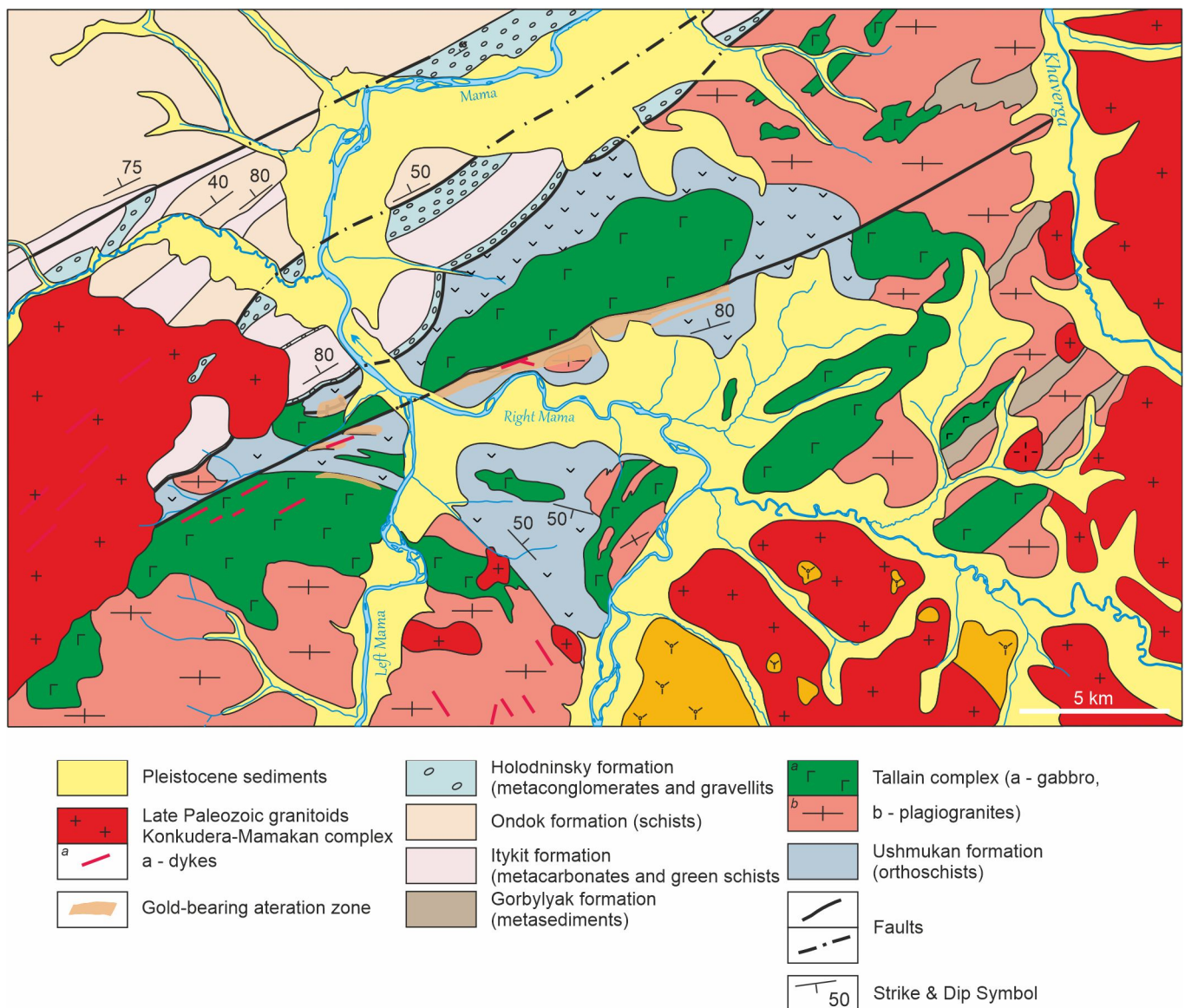


Figure 11. Geological map of the Mukodek orefield (after [25]).

Ore mineralisation is represented by two types of formation: sulphide lead-zinc and siderite ores. The main ore minerals are pyrite, sphalerite and siderite and the minor minerals are galena and magnetite. Accessory minerals are native silver, native gold, pyrite, marcasite, etc. Two main paragenetic associations are known in the deposit: galena-sphalerite-pyrite and siderite [30]. Two generations of pyrite have been identified. Pyrite-1 is represented by collomorphic aggregates 0.01–1 mm in size. This pyrite contains sphalerite and galena (Figure 8g,h). Pyrite-2 is represented by angular and cubic forms of various sizes and has inclusions of gold and silver. Although these metals are not in economic quantities, the study of the Ozernoye deposit adds to the understanding of the genesis of gold deposits in Transbaikalia.

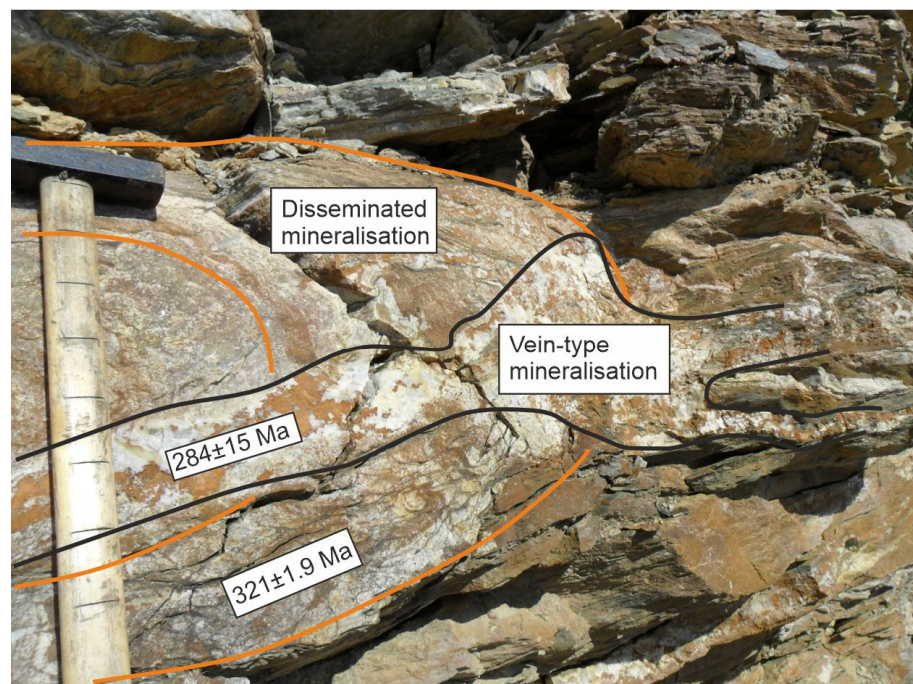


Figure 12. Geological relationship of veins and disseminated ore types at the Mukodek ore-field.

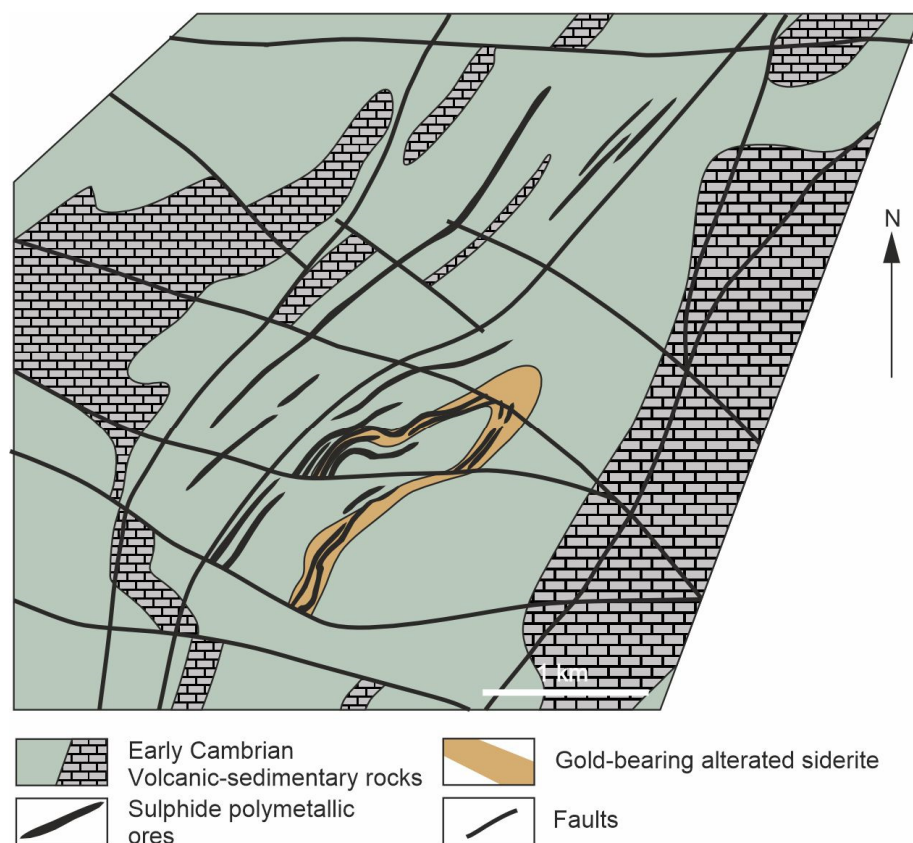


Figure 13. Geological map of the Ozernoe deposit (modified after [26]).

3. Methods

Based on the study of the geological structure, pyrite samples were collected from quartz veins at the Yubileinoe, Uryakh and Irokinda deposits for $^{40}\text{Ar}/^{39}\text{Ar}$ dating. At the Ozernoe deposit, pyrite-1 was collected, which is common in sulphide polymetallic ores of the disseminated type. The samples examined, therefore, represent a particular stage in the formation of the deposit. Pyrite-1 from some deposits did not contain significant amounts of sericite inclusions and did not give an analytical signal for ^{40}Ar . These are not discussed in the paper. Pyrite grains of each generation were mounted in epoxy, polished, coated with carbon and analysed using an LEO electron microscope with an INCA Energy 300 energy dispersive spectrometer at the Institute of Geology, Siberian Branch, Russian Academy of Sciences, Ulan-Ude, Russia. The analysed pyrites contain inclusions of sericite and gold (Figure 8).

The $^{40}\text{Ar}/^{39}\text{Ar}$ dating procedure has been described in detail by [4]. Briefly, the dating was carried out at the Centre for Geodynamics and Geochronology of the Institute of the Earth's Crust, Siberian Branch of the Russian Academy of Sciences (Irkutsk, Russia). The instrument used was an ARGUS VI noble gas mass spectrometer (Thermo Fisher Scientific, Waltham, MA, USA) equipped with a double vacuum resistance furnace and an SAES gas purification system. Argon was released using the stepwise heating procedure in 8–10 steps, depending on the amount of radiogenic argon in the dated pyrite samples. Ages were calculated using conventional decay constants [31] relative to an age of 18.885 Ma for the BERN 4M standard. Stepwise heating plots were plotted using Isoplot macros for Excel [32] and redrawn for aesthetic purposes (Figure 14). The original data in Excel format are provided in a supplementary file.

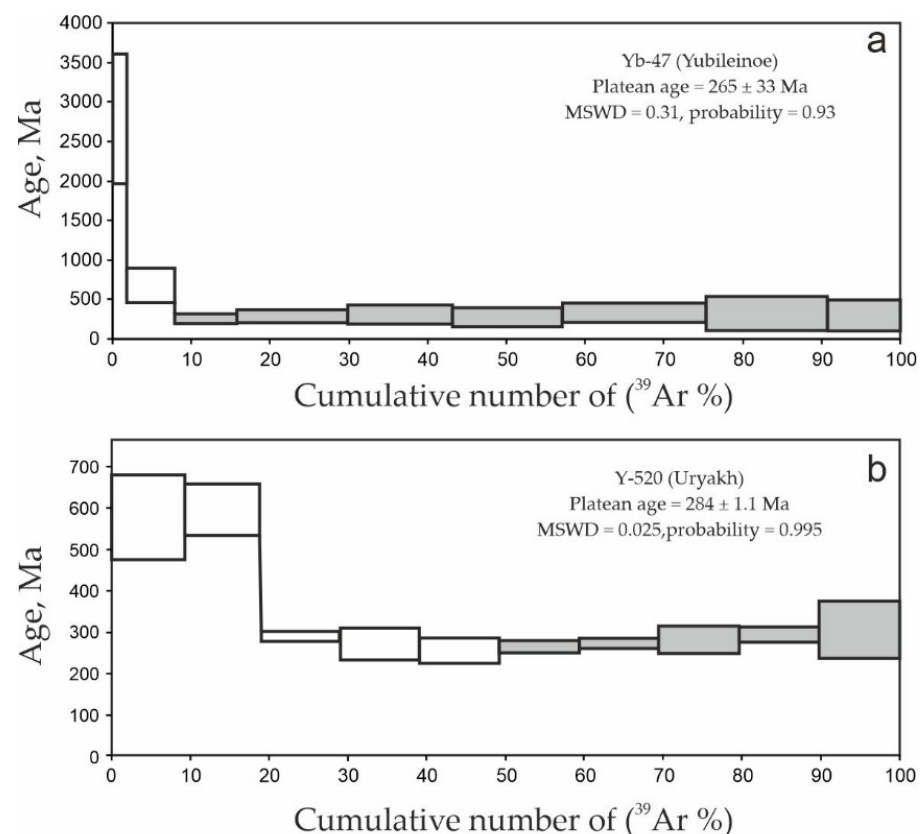


Figure 14. Cont.

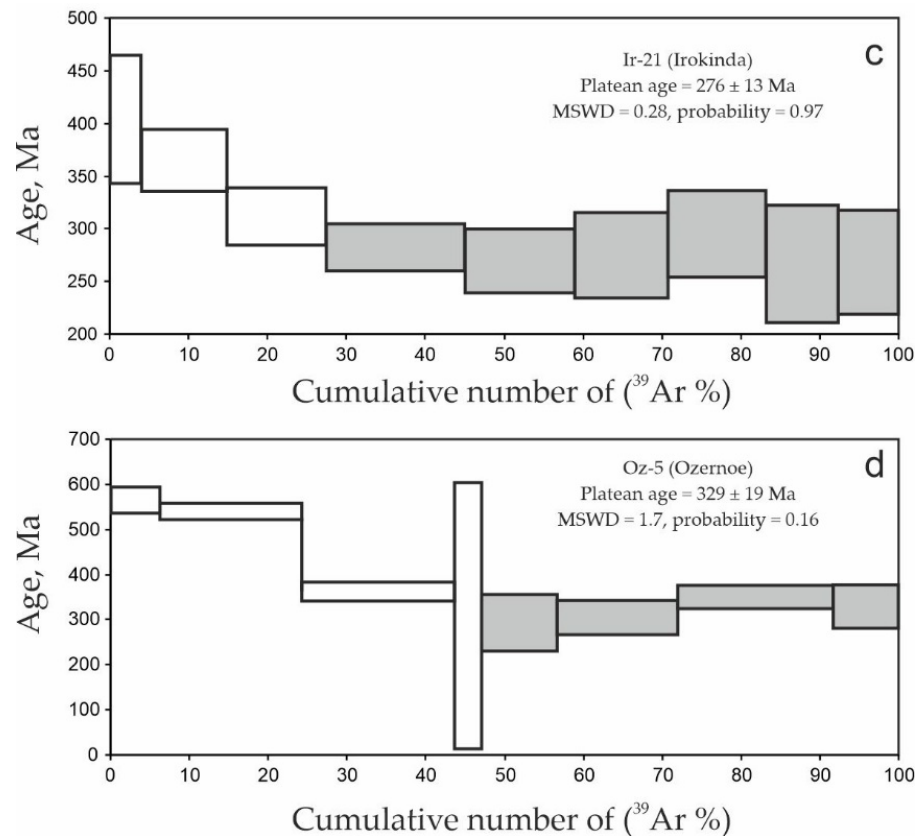


Figure 14. $^{40}\text{Ar}/^{39}\text{Ar}$ stepwise-heating diagrams: (a) Yubileinoe deposit; (b) Uryakh deposit; (c) Irokinda deposit; (d) Ozernoe deposit. Plateau segments used for the age calculation are shaded.

4. Results

Each of the four dated samples yielded a number of steps within their analytical uncertainties (plateau), with more than 50% of the released ^{39}Ar (Figure 14a–d). Following our previous study [4], we interpret such plateaus as ages of pyrite-encapsulated sericite crystallisation. A summary of the results is given in Table 1 and Figure 14. Namely, sample Yb-47 (Yubileinoe deposit)—7 out of 9 steps give an age of 265 ± 33 Ma (MSWD = 0.31, probability of fit 0.93); sample Y-520 (Uryakh deposit)—7 out of 10 steps give an age of 284 ± 1.1 Ma (MSWD 0.025, probability of fit 0.995); sample Ir-21 (Irokinda deposit)—6 out of 9 steps give an age of 276 ± 13 Ma (MSWD = 0.28, probability of fit 0.97); and sample Oz-5 (Ozernoe deposit)—4 of 8 steps yield an age of 329 ± 19 Ma (MSWD = 1.7, probability of fit 0.16). This last sample is characterised by an MSWD greater than one and a low probability of fit, so this age is only a preliminary estimate. The other three samples, from three different deposits, give ages within the analytical uncertainties.

Table 1. Characteristics of the Transbaikalian deposits.

Deposits, Tonnage	Neoproterozoic Host Rocks	Mineral Assemblages	Type	Ore Mineralisation	Age, Ma	Method	Reference
Yubileinoe, 25 tonn	Metavolcanic	Quartz vein (quartz, carbonate/pyrite, galena, sphalerite, chalcopyrite, gold-silver tellurides, native gold)	Au	Vein-type	265 ± 33	$^{40}\text{Ar}/^{39}\text{Ar}$	(This study)
Uryakh, 10 tonnes	Terrigenous carbonate Granitoids Gabbro	Quartz vein and sulfide disseminated mineralization (quartz, carbonate/pyrite, galena, sphalerite, chalcopyrite, fahlores, scheelite, goldsilver tellurides, native gold)	Au	Vein-type Vein-type Vein-type	275 ± 6 281 ± 5 284 ± 1	$^{40}\text{Ar}/^{39}\text{Ar}$ Rb-Sr $^{40}\text{Ar}/^{39}\text{Ar}$	[18] [18] (This study)

Table 1. Cont.

Deposits, Tonnage	Neoproterozoic Host Rocks	Mineral Assemblages	Type	Ore Mineralisation	Age, Ma	Method	Reference
Irokinda, 24 tonnes	Gneisses Granitoids	Quartz vein (quartz, carbonate/pyrite, galena, sphalerite, chalcopyrite, fahlores, scheelite, native gold)	Au	Vein-type Vein-type Vein-type Vein-type	271 ± 5 275 ± 7 268 ± 5 276 ± 13	K-Ar Rb-Sr $^{40}\text{Ar}/^{39}\text{Ar}$ $^{40}\text{Ar}/^{39}\text{Ar}$	[20] [20] [21] (This study)
Ozernoe, 165 M tonnes	Metavolcanic	sulphide lead-zinc and siderite ores (galena-sphalerite-pyrite)	Au-Pb-Zn	Disseminated-type	329 ± 19	$^{40}\text{Ar}/^{39}\text{Ar}$	(This study)
Mukodek ore field, 20 tonnes	Metavolcanic Plagiogranits	Quartz vein and sulfide disseminated mineralization quartz/pyrite, galena, sphalerite, halcopyrite, gold- silver tellurides, native gold)	Au	Disseminated-type Vein-type	321 ± 2 284 ± 15	$^{40}\text{Ar}/^{39}\text{Ar}$ $^{40}\text{Ar}/^{39}\text{Ar}$	[4] [4]
Kedrovskoe, 28 tonnes	Metasedimentary rocks, Gabbroids, Granitoids	Quartz vein (quartz, carbonate/pyrite, galena, sphalerite, pyrrhotite, chalcopyrite, fahlores, scheelite, native gold)	Au	Vein-type	273 ± 4 282 ± 5	Rb-Sr K-Ar	[24] [20]

5. Discussion

Previously, K-Ar dating of deposits on the southern periphery of the Siberian Craton suggested late Palaeozoic mineralisation [20]. The $^{40}\text{Ar}/^{39}\text{Ar}$ age of the metasomatic rock sericite from the Uryakh deposit is 275 ± 6 Ma, and from the Irokinda deposit is 268 ± 5 Ma [18,21]. Our studies carried out at the Transbaikalia deposits allowed us to determine that the quartz vein type of ores intersect the structural pattern (schistosity) of the disseminated ores (Figures 3, 6 and 12). This fact indicates that the formation of alteration zones (Au and Pb-Zn ores) in the Transbaikalia are took place in at least two main tectonic stages. The first stage is associated with the formation of ore-controlling faults and alteration of the host rocks. The first stage produced disseminated ore types. These ore types have acquired a structural pattern (schistosity) inherited from the ore-controlling faults. As the faults continued to “work”, the disseminated ores were deformed into various asymmetric folds (Figures 3 and 12). The first stage is associated with the formation of ore-controlling faults and alteration of the host rocks, resulting in the formation of the disseminated ores.

In the second stage, the ore-controlling faults were reactivated, resulting in the formation of new quartz-filled fractures that formed a quartz vein type of ore. In certain areas of the deposit, these new quartz-filled fractures either intersected or conformed to the schistosity of the veined ore. In areas where the quartz-filled fractures have adapted to the structural pattern of the disseminated ores, a false impression is created that the quartz vein and disseminated ores formed during the same tectonic stage.

The $^{40}\text{Ar}/^{39}\text{Ar}$ ages obtained for pyrites from the disseminated ores of the Ozernoe and Mukodek deposits are 329 ± 19 Ma and 321 ± 2 Ma, respectively. These, in our opinion, reflect the age of the first stage of tectonic activation (including the formation of ore-controlling faults) and the formation of Au and Pb-Zn (Ozernoe) vein-disseminated and disseminated ores.

$^{40}\text{Ar}/^{39}\text{Ar}$ ages of 265 ± 33 Ma, 287 ± 7 Ma, 276 ± 13 Ma and 284 ± 15 Ma were obtained for pyrites sampled from quartz veins of the Yubileinoe, Uryakh and Irokinda deposits and the Mukodek ore field. These data probably reflect the second stage of tectonic activation of ore-controlling faults and formation of vein-type ores. The processes responsible for gold formation continued for some time after the formation of the second-stage sulphide mineralisation, as evidenced by the occurrence of gold in the fractures of late pyrites from quartz veins (Figure 8f). The time interval between the two main stages of the alteration zone in the Transbaikalia area was approximately up to 40 million years.

We therefore propose as a working hypothesis that there were at least two stages in the formation of gold mineralisation at Transbaikalia, irrespective of the composition of the host rock and terrain attribution (Figure 1). The two stages are apparent from geological data and are supported by $^{40}\text{Ar}/^{39}\text{Ar}$ dating at the Mukodek ore field [4] and the Ozernoe deposit (this study), where in the first stage (~330–320 Ma) rocks in zones of

ore-controlling faults were locally subjected to metasomatic alteration. Disseminated gold mineralisation occurred in such zones. Later, the early metasomatic rocks were subjected to plastic deformation and medium-scale folds were formed. Gold-bearing quartz veins and quartz-carbonate veins were formed during the second stage (~270–290 Ma). It should be noted that younger (second stage) $^{40}\text{Ar}/^{39}\text{Ar}$ ages are only obtained on pyrite associated with vein-type ores (Table 1). The $^{40}\text{Ar}/^{39}\text{Ar}$ ages constrained for the ore deposits in our study correlate well with the period of geodynamic processes that caused the formation of the granitoids of the Angara-Vitim batholith with a size of ~200,000 km² (330–275 Ma) [5–8]. It should be noted that the Angara-Vitim batholith is a historical name and does not refer to granite emplacement in a single episode. In the interval of 330–310 Ma calcalkaline granites were emplaced, then between 305 and 285 Ma, in addition to calcalkaline, transitional to alkaline granitoids were emplaced, and finally at ~280–275 Ma, peralkaline and alkali feldspar syenites and granites were emplaced [7]. The batholith is thus composed of numerous separate intrusions emplaced over a long period of time with evolving chemical compositions. Each of these intrusions created its own hydrothermal system. The processes associated with the formation of granitoids provided a source of heat and possibly fluids for the mineral genesis system. Probably alkaline magmas provided more reactive fluids leading to a more productive stage of vein-type mineralisation. However, the source of gold was within the host rocks [26], as demonstrated by Pb isotopic studies of ores from the Mukodek ore field [33]. Carbonates are only significant in one deposit—Uryakh, which has the lowest gold resources (Table 1). The presence of interbedded terrigenous (gold-bearing) and carbonate (gold-free) rocks is probably the reason for the low tonnage. It is also clear that the age of gold and polymetallic deposits shifts from older to younger as one moves outwards from the Siberian Craton (Figure 1).

6. Conclusions

In this paper we have studied four deposits located in different terrains in the distribution area of the Early Carboniferous–Early Permian Angara-Vitim batholith. Within some of the deposits, two tectonic stages are identified, characterised by first- and second-generation pyrite. $^{40}\text{Ar}/^{39}\text{Ar}$ dating of pyrite-encapsulated sericite indicates that first-generation pyrite crystallized in the Early Carboniferous, whereas second-generation pyrite crystallized in the Early Permian. Thus, the formation of the deposits is temporally related to the emplacement of the Angara-Vitim batholith, which probably provided the heat to remobilise the ore metals. Gold deposits to the north and south of the batholith are generally older and younger, respectively, and were formed by different geological processes.

Supplementary Materials: The following are available online at <https://www.mdpi.com/article/10.3390/min14111158/s1>, Table S1: $^{40}\text{Ar}/^{39}\text{Ar}$ data in Excel format.

Author Contributions: V.A.V.; investigation and writing—original draft preparation. A.V.I.; project administration, methodology, writing—review and editing. A.E.B.; resources. V.A.G.; investigation and data curation. N.S.B.; funding acquisition, writing—review and editing. All authors have read and agreed to the published version of the manuscript.

Funding: This work was carried out with the financial support of a project from the Russian Federation represented by the Ministry of Education and Science of Russia (Project No. 13.1902.24.44, Agreement No. 075-15-2024-641).

Data Availability Statement: Data are contained within the article and Supplementary Materials.

Conflicts of Interest: The authors declare no conflicts of interest.

References

1. Smith, P.E.; Evensen, N.M.; York, D.; Moorbath, S. Oldest reliable terrestrial $^{40}\text{Ar}/^{39}\text{Ar}$ age from pyrite crystals at Isuawest Greenland. *Geophys. Res. Lett.* **2005**, *32*, L21318. [CrossRef]
2. Smith, P.E.; Evensen, N.M.; York, D.; Szatmari, P.; de Oliveira, D.C. Single crystal $^{40}\text{Ar}/^{39}\text{Ar}$ dating of pyrite: No fool's clock. *Geology* **2001**, *29*, 403–406. [CrossRef]

3. Phillips, D.; Miller, J.M. $^{40}\text{Ar}/^{39}\text{Ar}$ dating of mica-bearing pyrite from thermally overprinted Archean gold deposits. *Geology* **2006**, *34*, 397–400. [[CrossRef](#)]
4. Ivanov, A.V.; Vanin, V.A.; Demonterova, E.I.; Gladkochub, D.P.; Donskaya, T.V.; Gorovoy, V.A. Application of the ‘no fool’s clock’ to dating the Mukodek gold field, Siberia, Russia. *Ore Geol. Rev.* **2015**, *69*, 352–359. [[CrossRef](#)]
5. Yarmolyuk, V.V.; Budnikov, S.V.; Kovalenko, V.I.; Antipin, V.S.; Goreglyad, A.V.; Salnikova, E.B.; Kotov, A.B.; Kozakov, I.K.; Kovach, V.P.; Yakovleva, S.Z.; et al. Geochronology and geodynamic setting of the Angara–Vitim batholith. *Petrology* **1999**, *5*, 401–414.
6. Tsygankov, A.A.; Litvinovsky, B.A.; Jahn, B.M.; Reichow, M.K.; Liu, D.Y.; Larionov, A.N.; Presnyakov, S.L.; Lepekhina, Y.N.; Sergeev, S.A. Sequence of magmatic events in the Late Paleozoic of Transbaikalia, Russia (U–Pb isotope data). *Russ. Geol. Geophys.* **2010**, *51*, 972–994. [[CrossRef](#)]
7. Litvinovsky, B.A.; Tsygankov, A.A.; Jahn, B.M.; Katzir, Y.; Be’eri-Shlevin, Y. Origin and evolution of overlapping calc-alkaline and alkaline magmas: The Late Palaeozoic post-collisional igneous province of Transbaikalia (Russia). *Lithos* **2011**, *125*, 845–874. [[CrossRef](#)]
8. Donskaya, T.V.; Gladkochub, D.P.; Mazukabzov, A.M.; Ivanov, A.V. Late Paleozoic—Mesozoic subduction-related magmatism at the southern margin of the Siberian continent and the 150-million-year history of the Mongolia–Okhotsk Ocean. *J. Asian Earth Sci.* **2013**, *62*, 79–97. [[CrossRef](#)]
9. Rytsk, E.Y.; Kovach, V.P.; Yarmolyuk, V.V.; Kovalenko, V.I.; Bogomolov, E.S.; Kotov, A.B. Isotopic structure and evolution of the continental crust in the East Transbaikalian segment of the Central Asian foldbelt. *Geotectonics* **2011**, *45*, 349–377. [[CrossRef](#)]
10. Chugaev, A.V.; Budyak, A.E.; Larionova, Y.O.; Chernyshev, I.V.; Travin, A.V.; Tarasova, Y.I.; Gereev, B.I.; Batalin, G.A.; Rassokhina, I.V.; Oleinikova, T.I. ^{40}Ar – ^{39}Ar and Rb–Sr age constraints on the formation of Sukhoi–Log-style orogenic gold deposits of the Bodaibo District (Northern Transbaikalia, Russia). *Ore Geol. Rev.* **2022**, *144*, 104855. [[CrossRef](#)]
11. Laverov, N.P.; Chernyshev, I.V.; Chugaev, A.V.; Bairova, E.D.; Gol’tsman, Y.V.; Distler, V.V.; Yudovskaya, M.A. Formation stages of the large-scale noble metal mineralization in the Sukhoi Log deposit, east Siberia: Results of isotope-geochronological study. *Dokl. Earth Sci.* **2011**, *415*, 810–814. [[CrossRef](#)]
12. Vanin, V.A.; Mazukabzov, A.M.; Yudin, D.S.; Blinov, A.V.; Tarasova, Y.I. The Hercynian imposed deformations in the Golets Vysochaishii deposit structure (Baika–Patom belt), $^{40}\text{Ar}/^{39}\text{Ar}$ data. *Geodyn. Tectonophys.* **2022**, *13*, 0575. [[CrossRef](#)]
13. Yudovskaya, M.A.; Distler, V.V.; Mokhov, A.V.; Rodionov, N.V.; Antonov, A.V.; Sergeev, S.A. Relationship between metamorphism and ore formation at the Sukhoi Log gold deposit hosted in black slates from the data of U–Th–Pb isotopic SHRIMP-dating of accessory minerals. *Geol. Ore Depos.* **2011**, *53*, 27–57. [[CrossRef](#)]
14. Zorin, Y.u.A.; Zorina, L.D.; Spiridonov, A.M.; Rutshtein, I.G. Geodynamic setting of gold deposits in Eastern and Central Trans-Baikal (Chita Region, Russia). *Ore Geol. Rev.* **2001**, *17*, 215–232. [[CrossRef](#)]
15. Spiridonov, A.N.; Zorina, L.D.; Kitayev, N.A. *Gold-Bearing Ore-Magmatic Systems of Transbaikalia*; Geo: Novosibirsk, Russia, 2006; p. 291.
16. Zhilyaeva, A.I.; Naumov, V.B.; Kudryavtseva, G.P. Mineral composition and fluid regime of formation of the Yubileinoe gold deposit (Transbaikalia, Russia). *Geol. Ore Depos.* **2000**, *42*, 63–73.
17. Chugaev, A.V.; Vanin, V.A.; Chernyshev, I.V.; Shatagin, K.N.; Rassokhina, I.V.; Sadasyuk, A.S. Lead isotope systematics of the orogenic gold deposits of the Baikal–Muya Belt (Northern Transbaikalia): Contribution of the subcontinental lithospheric mantle in their genesis. *Geochem. Int.* **2022**, *60*, 1352–1379. [[CrossRef](#)]
18. Chugaev, A.V.; Nosova, A.A.; Abramov, S.S.; Chernyshev, I.V.; Bortnikov, N.S.; Larionov, Y.O.; Goltsman, G.V.; Volfson, A.A. Early Permian stage of formation of gold-ore deposits of northeastern Transbaikalia: Isotope-geochronological (Rb–Sr and ^{40}Ar – ^{39}Ar) data for the Uryakh ore field. *Dokl. Earth Sci.* **2015**, *463*, 855–859. [[CrossRef](#)]
19. Namolov, E.A. Tectonic conditions of formation and patterns of morphology of ore-bearing fractures of the Irokinda ore field. In *Tectonic Structures and Patterns of Distribution of Minerals on the Territory of Transbaikalia*; Buryat Branch of the Siberian Division of the Academy of Sciences of the Soviet Union: Ulan-Ude, Russia, 1979; pp. 70–79.
20. Kucherenko, I.V. Late Paleozoic epoch of gold mineralization in the Precambrian frame of the Siberian platform. *News of the USSR Academy of Sciences. Geol. Ser.* **1989**, *6*, 90–102.
21. Chugaev, A.V.; Dubinina, E.O.; Chernyshev, I.V.; Kossova, S.A.; Larionova, Y.O.; Nosova, A.A.; Plotinskaya, O.Y.; Oleinikova, T.I.; Sadasyuk, A.S.; Travin, A.V. Sources and age of the gold mineralization of the Irokinda deposit, northern Transbaikalia: Evidence from Pb, S, Sr, and Nd isotope-geochemical and ^{39}Ar – ^{40}Ar geochronological data. *Geochem. Int.* **2020**, *58*, 1208–1227. [[CrossRef](#)]
22. Rytsk EYu Amelin, Y.u.V.; Rizvanova, N.G.; Krinsky RSh Mitrofanov, G.L.; Mitrofanova, N.N.; Perelyaev, V.I.; Shalaev, V.S. Age of rocks in the Baikal–Muya foldbelt. *Stratigr. Geol. Correl.* **2001**, *9*, 315–326.
23. Gusev, G.S.; Khain, V.E. On the relationships of the Baikal–Vitim, Aldan–Stanovoy and Mongol–Okhotsk terranes (south of Central Siberia). *Geotectonics* **1995**, *5*, 68–82.
24. Chugaev, A.V.; Plotinskaya, O.Y.; Chernyshev, I.V.; Lebedev, V.A.; Belogub, E.V.; Goltsman, Y.V.; Larionova, Y.O.; Oleinikova, T.I. Age and sources of matter for the Kedrovskoe gold deposit, northern Transbaikalia Region, Republic of Buryatia: Geochronological and isotopic geochemical constraints. *Geol. Ore Depos.* **2017**, *59*, 281–297. [[CrossRef](#)]

25. Vanin, V.A.; Tatarinov, A.V.; Gladkochub, D.P.; Mazukabzov, A.M.; Molochnuy, V.G. The role of dynamometamorphism in the formation of the Mukodek gold field (North Pribaikalie). *Geodyn. Tectonophys.* **2017**, *8*, 643–653. [[CrossRef](#)]
26. Kovalev, K.R.; Ripp, G.S.; Distanov, E.G.; Baulina, M.V. Ferruginous-magnesian carbonates and variations of carbon and oxygen isotopes at the hydrothermal-sedimentary pyrite-polymetallic Ozeroye deposit (Transbaikalia). *Russ. Geol. Geophys.* **2005**, *46*, 383–397.
27. Gordienko, I.V. Strategic mineral resources of the Republic of Buryatia: Status and prospects of development. *Earth Sci. Subsoil Use* **2020**, *43*, 8–35. [[CrossRef](#)]
28. Vasiliev, I.L. *Geology of the Yeravninsky Ore Field*; Nauka: Novosibirsk, Russia, 1977; p. 126.
29. Tsarev, D.I.; Firsov, A.P. *The Problem of the Formation of Pyrite Deposits (on the Example of Transbaikalia)*; Science Publisher: Moscow, Russia, 1988; p. 144.
30. Distanov, E.G.; Kovalev, K.R.; Tarasova, R.S. Geological structure and genesis of the Ozerne lead-zinc pyrite deposit (Western Transbaikalia). *Geol. Ore Depos.* **1972**, *14*, 3–22.
31. Steiger, R.H.; Jäger, E. Subcommission on geochronology: Convention on the use of decay constants in geo- and cosmochronology. *Earth Planet. Sci. Lett.* **1977**, *6*, 359–362. [[CrossRef](#)]
32. Ludwig, K.R. ISOPLOT 3.75. A geochronological toolkit for Microsoft Excel. *Berkeley Geochronol. Cent. Spec. Publ.* **2012**, *5*, 75.
33. Vanin, V.A.; Chugaev, A.V.; Demonterova, E.I.; Gladkochub, D.P.; Mazukabzov, A.M. Geological structure of the Mukodek gold-ore field, Northern Transbaikalia and material sources (Pb-Pb and Sm-Nd data). *Russ. Geol. Geophys.* **2018**, *59*, 1078–1086. [[CrossRef](#)]

Disclaimer/Publisher’s Note: The statements, opinions and data contained in all publications are solely those of the individual author(s) and contributor(s) and not of MDPI and/or the editor(s). MDPI and/or the editor(s) disclaim responsibility for any injury to people or property resulting from any ideas, methods, instructions or products referred to in the content.